Localized structures in dryland vegetation: Forms and functions

Ehud Meron, Hezi Yizhaq, and Erez Gilad

Citation: Chaos **17**, 037109 (2007); doi: 10.1063/1.2767246
View online: https://doi.org/10.1063/1.2767246
View Table of Contents: http://aip.scitation.org/toc/cha/17/3
Published by the American Institute of Physics

Localized structures in dryland vegetation: Forms and functions

Ehud Meron
Department of Solar Energy and Environmental Physics, BIDR, Ben-Gurion University, Sede Boqer Campus, 84990, Israel and Physics Department, Ben-Gurion University, Beer-Sheva, 84105, Israel

Hezi Yizhaq
Department of Solar Energy and Environmental Physics, BIDR, Ben-Gurion University, Sede Boqer Campus, 84990, Israel

Erez Gilad
School of Biological Sciences, Royal Holloway, University of London, Egham, Surrey, TW20 0EX, United Kingdom

(Received 2 March 2007; accepted 9 July 2007; published online 28 September 2007)

Vegetation patches in drylands are localized structures of biomass and water. We study these structures using a mathematical modeling approach that captures biomass-water feedbacks. Biomass-water structures are found to differ in their spatial forms and ecological functions, depending on species type, soil conditions, precipitation range, and other environmental factors. Asymptotic spot structures can destabilize to form ring structures, expanding in the radial direction, or crescent structures, migrating uphill. Stable spot structures can differ in their soil-water distributions, forming water-enriched patches or water-deprived patches. The various biomass-water structures are expected to function differently in the context of a plant community, forming landscapes of varying species diversity. © *2007 American Institute of Physics*.
[DOI: 10.1063/1.2767246]

Vegetation patches surrounded by bare soil are common vegetation forms in dryland landscapes.[1] They form localized structures of biomass and soil-water that vary in size, spatial shape, and function. Vegetation patches can be as small as a few centimeters in diameter (perennial grasses) or as big as a few tens of meters (trees). They can assume spot, ring or crescent shapes, and can deplete the limiting water resource or concentrate it to form habitats for other species. Using a mathematical modeling approach, we study the conditions that give rise to vegetation patches of different shapes, and the roles these patches play in modifying the spatial distribution of the limiting water resource. Among our findings are a crossover from water-deprived to water-rich patches as the aridity of the system increases, and an instability of spots to rings associated with the root-system size. The results presented here shed new light on the processes of species-diversity change in arid and semiarid regions.

I. INTRODUCTION

Recent model studies of dryland vegetation[2–11] support the view of vegetation pattern formation as a symmetry breaking phenomenon,[12] induced by water stress. These studies predict the appearance of five basic vegetation states along the rainfall gradient: uniform vegetation, gap pattern, stripe pattern, spot pattern, and bare soil. They also predict rainfall ranges where two or more different stable vegetation states coexist. The five basic states along with their multistability ranges provide a wide variety of vegetation patterns, many of which have been observed in the field.[13–15] Among these patterns are sparse vegetation patches surrounded by bare soil, which are the subject of this paper.

Vegetation pattern formation has been attributed to positive feedback processes involving plant biomass and water.[6,7,9,11] One process of this kind is associated with increased infiltration rates at vegetation patches; as the plants comprising a vegetation patch grow they often modify the local biotic and abiotic environments in ways that increase the infiltration rate of surface water into the soil.[16] The increased infiltration rate at a vegetation patch leads to surface-water flow into the patch which increases the soil-water content there, and accelerates plant growth. Another positive feedback is water uptake by root systems that grow in size in response to plant growth. By probing new, unexploited soil regions, these root systems increase the amount of soil-water available to the plants, thereby accelerating their growth. Both processes accelerate plant growth within vegetation patches and inhibit it in the surrounding bare soil.

The two feedbacks have opposing effects on the water balance in vegetation patches; while the infiltration feedback acts to concentrate soil-water in a patch, the uptake feedback acts to deplete it. Depending on the relative strengths of these feedbacks, localized structures that differ in form and function are expected to be found. Dominance of the uptake feedback is likely to favor species competition and exclusion, while dominance of the infiltration feedback may favor facilitation and coexistence. Surprisingly, despite the extensive study of vegetation patches in water-limited systems, and the interactions among the plant species comprising them, very little is known about the soil-water distributions in these patches.[17]

TABLE I. Relations between the nondimensional variables and parameters appearing in Eqs. (1)–(4) and their dimensional counterparts. The quantities B and W are the dimensional biomass and soil-water densities in units of $(\mathrm{kg/m^2})$, H is the dimensional height of the water layer above ground level in units of mm, and all other dimensional quantities are defined in Table II.

Quantity	Scaling	Quantity	Scaling
b	B/K	p	$\Lambda P/MN$
w	$\Lambda W/N$	δ_b	D_B/MS_0^2
h	$\Lambda H/N$	δ_w	D_W/MS_0^2
q	Q/K	δ_h	$D_H N/M\Lambda S_0^2$
ν	N/M	ζ	$\Lambda Z/N$
α	A/M	ρ	R
η	EK	t	MT
γ	$\Gamma K/M$	$\mathbf{x}$	$\mathbf{X}/S_0$

In this paper we use a mathematical modeling approach to study biomass and soil-water distributions associated with vegetation patches of a single plant species. We study the relative strength of the infiltration and uptake feedbacks at various environmental conditions and discuss the implications of the resulting water-biomass distributions on ecosystem engineering, species diversity, and desertification. This is a synthetic review of earlier results,[9–11,18] complemented by new results related to patch-form instabilities.

II. A DYNAMIC MODEL FOR WATER-LIMITED VEGETATION

In earlier studies[9,11] we developed model equations to describe vegetation dynamics in water-limited systems. The model equations in nondimensional form are

$$b_t = G_b b(1-b) - b + \delta_b \nabla^2 b,$$

$$w_t = \mathcal{I}h - \nu(1-\rho b)w - G_w w + \delta_w \nabla^2 w, \tag{1}$$

$$h_t = p - \mathcal{I}h + \delta_h \nabla^2 h^2 + 2\delta_h \nabla h \cdot \nabla \zeta + 2\delta_h h \nabla^2 \zeta,$$

where $b(\mathbf{x},t)$ represents the areal density of overground vegetation biomass, $w(\mathbf{x},t)$ represents the areal soil-water density, and $h(\mathbf{x},t)$ is the height of a thin water layer above the ground level described by a prescribed topography function $\zeta(\mathbf{x})$ [where $\mathbf{x}=(x,y)$]. The relations between the nondimensional quantities appearing in (1) and their dimensional counterparts are given in Table I. The definitions of the latter and their units are given in Table II. Noteworthy is the nondimensional precipitation parameter p, which shows the equivalence of increasing the precipitation rate P and decreasing the biomass-loss rate M. Depending on the plant life-form to be considered we will assume constant or time-periodic forms for the precipitation parameter, representing mean annual rainfall rate or seasonal rainfall variations.

The model captures various feedback processes involving biomass growth, root augmentation, water uptake, and water evaporation, as described below.[19] The relative strengths of these processes determine the forms and functions of localized vegetation patches.

Infiltration feedback. This is a positive feedback between biomass and water due to increased infiltration rates of surface water into the soil in vegetation patches. The feedback is captured by the following terms in the model equations: (a) the term $\mathcal{I}h$ in the equation for w, where the infiltration rate $\mathcal{I}$ is given by[20]

$$\mathcal{I}(\mathbf{x},t) = \alpha \frac{b(\mathbf{x},t) + qf}{b(\mathbf{x},t) + q}, \tag{2}$$

(b) the water-dependent biomass growth rate, G_b [see Eq. (3)], and (c) the water flow terms in the equation for h, parameterized by the nondimensional friction coefficient δ_h. A typical form of $\mathcal{I}$ is shown in Fig. 1. For $f<1$, the infiltration rate increases monotonically with the biomass density. As a result, higher biomass densities imply higher soil-water densities and therefore higher biomass-growth rates. The strength of this feedback can be controlled by the pa-

TABLE II. Definitions of dimensional model quantities and their units.

Parameter	Units	Description
K	$\mathrm{kg/m^2}$	Maximum standing biomass
Q	$\mathrm{kg/m^2}$	Biomass reference value beyond which infiltration rate under a patch approaches its maximum
M	$\mathrm{yr^{-1}}$	Rate of biomass loss due to mortality and disturbances
A	$\mathrm{yr^{-1}}$	Infiltration rate in fully vegetated soil
N	$\mathrm{yr^{-1}}$	Soil-water evaporation rate
E	$(\mathrm{kg/m^2})^{-1}$	Relative root's extension per unit biomass density
Λ	$(\mathrm{kg/m^2})^{-1}\ \mathrm{yr^{-1}}$	Biomass growth rate per unit soil-water density
Γ	$(\mathrm{kg/m^2})^{-1}\ \mathrm{yr^{-1}}$	Soil-water consumption rate per unit biomass density
D_B	$\mathrm{m^2/yr}$	Seed dispersal coefficient
D_W	$\mathrm{m^2/yr}$	Transport coefficient for soil water
D_H	$\mathrm{m^2/yr\ (kg/m^2)^{-1}}$	Bottom friction coefficient between surface water and ground surface
S_0	m	Minimal root length
$Z(\mathbf{X})$	mm	Topography function
P	$\mathrm{kg/m^2\ yr^{-1}}$	Precipitation rate
R	⋯	Evaporation reduction due to shading
f	⋯	Infiltration contrast between bare soil and vegetated soil

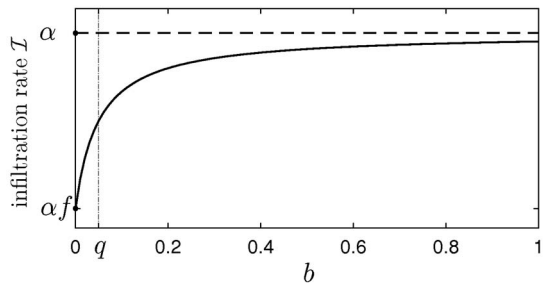

FIG. 1. The infiltration rate $\mathcal{I}$ as a function of biomass density b. The infiltration contrast between bare and vegetated soil is quantified by the parameter f, where $0<f<1$; when $f=1$ the contrast is zero and when $f=0$ the contrast is maximal. Note the weak dependence of the infiltration rate on biomass for $b \gg q$. Reprinted from Ref. 11. Copyright (2007), with permission from Elsevier.

rameter f. Lower values of f, modeling, e.g., the existence of biogenic crusts,[21] correspond to lower infiltration rates in bare soil relative to the infiltration rates in vegetation patches. This infiltration contrast increases the surface water flow towards the vegetation patches, and thereby strengthens the infiltration feedback.

Root-augmentation feedback. This is a positive feedback between the overground biomass and the underground roots. As the plant grows its root system extends in size and probes new soil regions where water can be taken up. As a result the amount of water available to the plant increases and the plant grows even further. This feedback is captured by the nonlinear and nonlocal form of the biomass growth rate

$$G_b(\mathbf{x},t) = \nu \int_\Omega g(\mathbf{x},\mathbf{x}',t) w(\mathbf{x}',t) d\mathbf{x}',$$
$$g(\mathbf{x},\mathbf{x}',t) = \frac{1}{2\pi} \exp\left[- \frac{|\mathbf{x}-\mathbf{x}'|^2}{2(1+\eta b(\mathbf{x},t))^2} \right], \tag{3}$$

where the integration is over the entire physical domain Ω. The Gaussian kernel g represents the root system whose size (width of the Gaussian) grows as the biomass density b grows. The strength of this feedback is quantified by the parameter η; the larger η the stronger the feedback. Larger η values represent species that allocate more resources to root growth.

Uptake feedback. This is a negative feedback between biomass and water due to water-uptake by the plant's roots. The depletion of soil-water at any given point is due to all plants whose roots extend to this point. The feedback is captured by the term $-G_w w$ in the equation for w, where the water consumption rate, G_w, increases with the biomass density according to

$$G_w(\mathbf{x},t) = \gamma \int_\Omega g(\mathbf{x}',\mathbf{x},t) b(\mathbf{x}',t) d\mathbf{x}'. \tag{4}$$

Shading feedback: This is a positive feedback between biomass and soil-water due to reduced evaporation at vegetation patches. The feedback is captured by the biomass dependence of the evaporation term, $-\nu(1-\rho b)w$, in the equation for w. Unlike the infiltration feedback, the increase of soil-water content under a vegetation patch does not involve the depletion of soil-water from the surroundings of the patch.

III. EXTENDED VEGETATION STATES

We consider in this section solutions of Eqs. (1)–(4) for constant values of the precipitation parameter p, representing mean annual rainfall rates. This approximation is valid for species such as woody plants whose growth-time scales are much longer than a year. The simplest solutions describe a stationary uniform bare-soil state and a stationary uniform-vegetation state, denoted in Fig. 2 by $\mathcal{B}$ and $\mathcal{V}$, respectively.

The bare soil solution is given by $b=0$, $w=p/\nu$, and $h=p/\alpha f$. It is linearly stable for $p<p_c=1$ and it loses stability at $p=1$ to uniform perturbations.[11,22] The uniform vegetation solution, $\mathcal{V}$, exists for $p>p_c=1$ in the case of a supercritical bifurcation and for $p>p_1$ (where $p_1<1$) in the case of a subcritical bifurcation. It is stable, however, only beyond another threshold, $p=p_2>p_1$ (outside the range shown in Fig. 2).

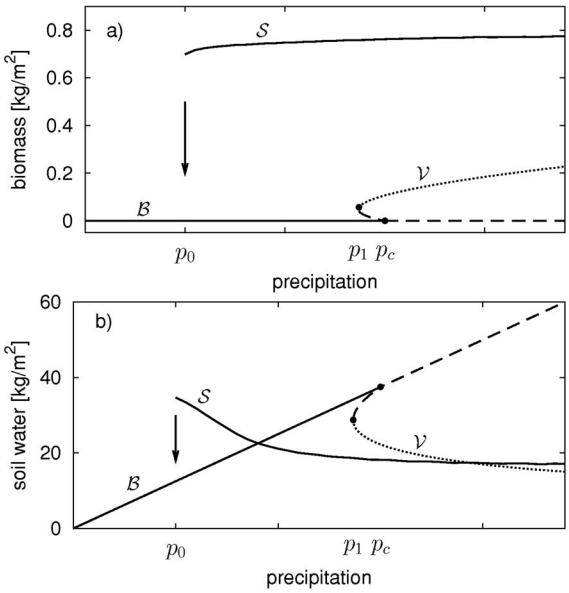

FIG. 2. Solution branches for the biomass and soil-water densities along the low end of the precipitation axis. The branches $\mathcal{B}$ and $\mathcal{V}$ denote, respectively, bare-soil and uniform-vegetation solutions. The branch $\mathcal{S}$ denotes a spot-pattern solution. In panel (a) it denotes the amplitude of the biomass density, while in panel (b) it denotes the soil-water density at the center of a biomass spot. The figure shows the coexistence range, $p_0<p<p_c$, of stable spot-pattern and bare-soil solutions, and illustrates the occurrence of a catastrophic shift (see arrow) as the precipitation drops below p_0. The $\mathcal{S}$ branch was calculated by numerical integration of the model equations [Eqs. (1)–(4)]. Parameters: $f=0.1$, $\nu=\delta_w=3.333$, $\alpha=33.333$, $q=0.05$, $\delta_h=333.333$, $\eta_1=3.5$, $\gamma_1=16.667$, $\rho_1=0.95$, and $\delta_b=0.033$.

As p is decreased below p_2 the uniform vegetation solution, $\mathcal{V}$, loses stability to nonuniform perturbations in a finite wave number (Turing-type) instability. These perturbations grow to form extended pattern states. The following sequence of basic pattern states has been found at decreasing precipitation values for plane topography:[9,11] hexagonal gap patterns, stripe patterns, and hexagonal spot patterns. The $\mathcal{S}$ branch in Fig. 2 shows the amplitude of the spot-pattern solution. Note the bistability range, $p_0<p<p_c$, of bare-soil ($\mathcal{B}$) and spot-pattern ($\mathcal{S}$) solutions. Bistability ranges exist for any other consecutive pair of states along the precipitation axis: spots and stripes, stripes and gaps, and gaps and uniform vegetation.

IV. LOCALIZED BIOMASS-WATER STRUCTURES

Localized structures often appear in bistability ranges of extended states.[23] Here we focus on the range $p_0<p<p_c$, where spot patterns and bare soil are both stable solutions of Eqs. (1)–(4). We take the precipitation parameter p to be a constant representing the mean annual rainfall rate. This restricts our consideration to plant species (e.g., woody) whose growth time scales are long in comparison to the seasonal time scale.

In the bistability range, $p_0<p<p_c$, we numerically find localized spot solutions representing isolated spot-like veg-

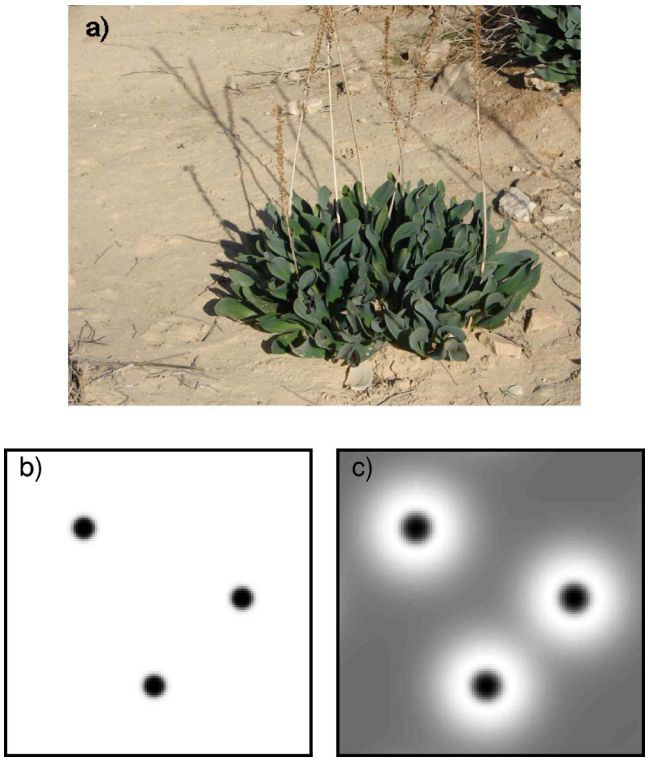

FIG. 3. Spot-like vegetation patches in the field (a) and as obtained by numerically solving Eqs. (1)–(4) (b), (c). Shown in (a) are patches of *Urginea maritima* observed in the Negev desert (80 mm/yr). (Photography by E. Meron.) Patch sizes are of the order of 40 cm. The spot solutions in (b) and (c) describe localized structures of biomass and soil water, respectively. Dark shades of gray represent high biomass or soil-water densities. Parameters (b), (c): $P=75$ mm/yr and all other parameters are as in Fig. 2. Domain sizes in (b), (c) are 7.5×7.5 m^2.

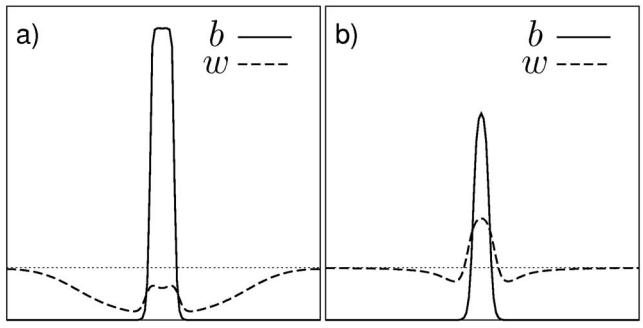

FIG. 4. Spatial profiles of the variables b and w as affected by the parameter that controls the root-augmentation feedback, η. The profiles are cross sections of two-dimensional spot solutions of the model Eqs. (1)–(4). The horizontal dotted lines denote the soil-water density at bare soil. A strong root-augmentation feedback ($\eta=5.5$) results in soil-water depletion (a). A weak root-augmentation feedback ($\eta=2$), and sufficiently strong infiltration feedback, leads to soil-water concentration (b). The domain size is 5 m. Values of all other parameters are as in Fig. 2 with $p=0.5$ (75 mm/yr).

etation patches in an otherwise bare-soil area. A solution representing such patches is shown in Figs. 3(b) and 3(c). Figure 3(a) shows a spot-like patch of *Urginea maritima* observed in the Negev desert. The stability of a localized spot structure stems from the depletion of the water resource in the immediate vicinity of the spot [see Fig. 3(c)] which prevents its further expansion. Contributing to this depletion process are the infiltration, root-augmentation, and uptake feedbacks. These feedbacks, together with the shading feedback, also determine the water balance within the spot, or under the vegetation patch it represents. In the following we study how this water balance is affected by species traits and by environmental changes.

Of the four feedbacks, the infiltration and shading feedbacks act to increase the soil-water content in a spot, whereas the uptake and root-augmentation feedbacks act to decrease it. Figure 4 shows the biomass and soil-water distributions in and around localized spot structures of species characterized by different values of the parameter η, which controls the strength of the root-augmentation feedback. When the root-augmentation feedback is strong (large η) the soil-water density in the spot and its vicinity is lower than in bare soil [Fig. 4(a)]. This solution represents a water-deprived patch, resulting from the high water-uptake by the large root systems in the patch. The water balance is inverted when the root-augmentation feedback is sufficiently weak (small η); the soil-water density in the spot area is larger than in bare soil [Fig. 4(b)], and the solution represents a water-enriched patch.

Water-enriched patches are obtained for small-η species (compact root systems) and small f values, representing strong infiltration contrasts between bare soil and vegetation patches (e.g., $f=0.1$ in Fig. 4). Such a situation is often realized in nature when the bare soil is covered by a biological crust.[21] What would be the effect of a disturbance that increases f, e.g., by removing the fragile crust? As Fig. 5 demonstrates, the general effect, at least for sufficiently high f values, is reduced soil-water content in the patch area because of increased infiltration in the surrounding bare soil. The strength of the root-augmentation feedback, however, is of critical importance. If this feedback is not strong enough (i.e. η large enough) a critical value, $f=f_c$, exists, beyond which the localized structure collapses to zero [down arrow in Fig. 5(a)]. A tradeoff therefore exists between the capability of a vegetation patch to concentrate the water resource and its resilience to disturbances.

Another possible consequence of increasing f from very low values is a change in the soil-water distribution in the patch area from a ringlike shape, where the highest density is at the patch periphery, to a spot-like shape, where the highest density is at the center of the patch. Such a change is seen in the small f range of Fig. 5(b). The mechanism of this change is related to the area occupied by the biomass spot (vegetation patch) which decreases as f increases. Bigger patches contain more individuals that compete for the water resource. The competition is strongest at the patch center and therefore acts to deplete the soil-water content there more than in other points of the patch. In addition, surface water flowing from the patch surrounding infiltrate mostly at the patch periphery, thereby increasing the soil-water content there as compared with the patch center.

A different type of environmental change, that may affect the water balance within a spot structure, is a precipitation downshift, such as a prolonged drought. As Fig. 6 demonstrates, at high precipitation rates ($p>p_f$) the soil-water

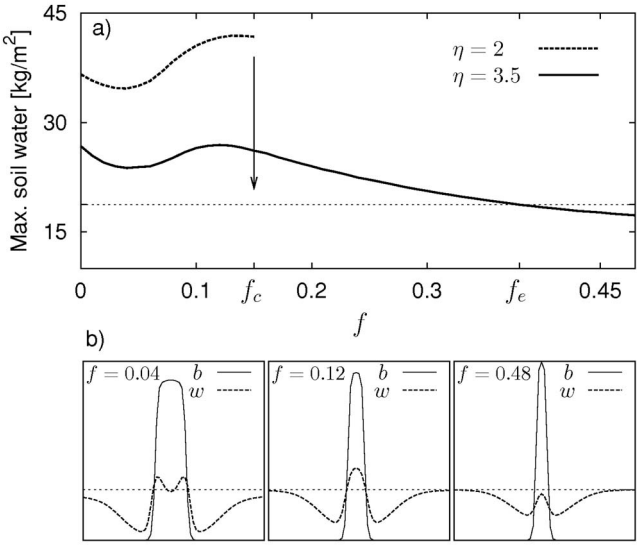

FIG. 5. Model calculations showing the effects of soil disturbances on spot-like vegetation patches. (a) The maximal soil-water density under a patch at increasing values of f (modeling e.g., gradual crust removal) for species characterized by η=2 (dashed line) and η=3.5 (solid line). The lower-η species concentrates more water but is not resilient to strong disturbances ($f > f_c$). The higher-η species is resilient to strong disturbances but loses the capability to concentrate soil-water when the disturbance is too strong ($f > f_e$). (b) Spatial profiles of b and w at increasing f values. In the small f range a ring-shape water distribution (f=0.04) changes into a spot-shape distribution (f=0.12). Parameters are as in Fig. 2 with p=0.5 (75 mm/yr). Reprinted [panel (a)] from Ref. 11. Copyright (2007), with permission from Elsevier.

density in the spot and its vicinity is lower than in bare soil, while at low precipitation rates ($p < p_f$) the soil-water density in the spot is higher than in bare soil. The mechanism of this crossover from water-deprived to water-enriched patches as a result of a precipitation downshift is again related to the patch size. At lower precipitation rates the patches are smaller, thus having fewer water-consuming plant individuals in any area element of the patch. The infiltration rate, on the other hand, is hardly reduced because of the weak dependence of the infiltration rate on biomass for grown-up plants (see Fig. 1).

Changes in patch structures, from water-deprived to water-enriched patches, or from ring-shape to spot-shape water distributions, have important implications for interspecific plant interactions and species diversity changes, as discussed in Sec. VI.

V. INSTABILITY TO RING AND CRESCENT STRUCTURES

Another common patch form observed in nature is the ring.[24–26] Figure 7 shows examples of ring-shape patches formed by different plant species in water-limited systems. Under what conditions do ringlike patches appear and how are these structures related to spot-like patches? In this section we use the model Eqs. (1)–(4) to study ring and crescent-like patch forms. Since rings have been observed with species spanning a wide range of growth rates, including fast growing herbaceous species, we study these

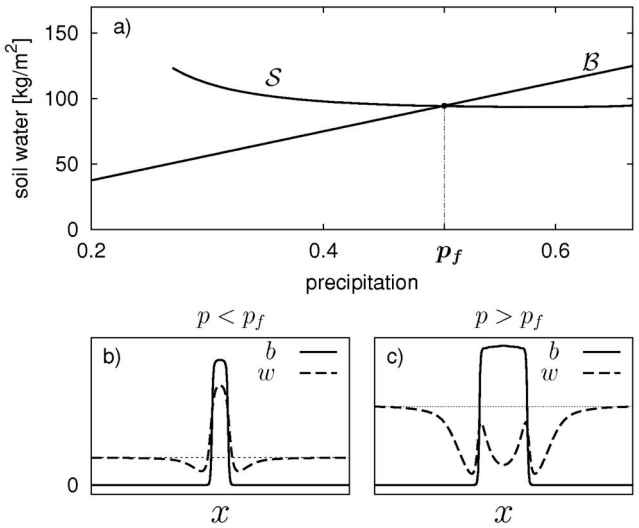

FIG. 6. A transition from water-deprived to water-enriched patches as a result of a precipitation down shift. The lines $\mathcal{B}$ and $\mathcal{S}$ in panel (a) show, respectively, the soil-water density in bare soil and the maximal soil-water density in a spot structure as functions of the precipitation rate p. Above (below) a crossover point, $p=p_f$, the water content in a spot structure is lower (higher) than in bare soil. Panels (b) and (c) show spatial profiles of b and w at precipitation rates below (187.5 mm/yr) and above (480 mm/yr) the crossover point p_f=0.504 which corresponds to 378 mm/yr. Parameters: $\nu=\delta_w$=1.667, α=16.667, q=0.05, f=0.1, δ_h=416.667, η=3.5, γ=2.083, ρ=0.95, δ_b=0.0167.

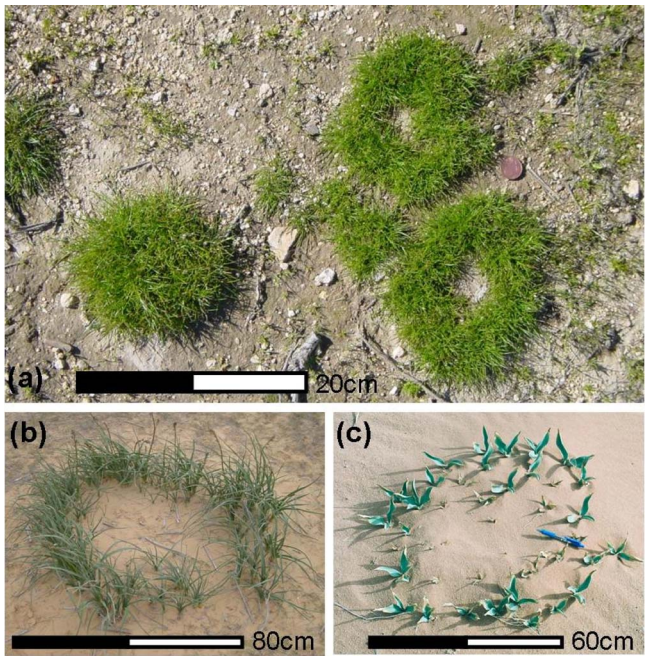

FIG. 7. Ring patterns in nature. (a) Mixture of rings and spots of Poa bulbosa observed in the Northern Negev (250 mm/yr). (b) A ring of *Asphodelus ramosus* observed in the Negev desert (170 mm/yr). (c) A ring of *Urginea maritima* observed in Wadi Rum, Jordan (50 mm/yr). Photography by J. von Hardenberg (a) and H. Yizhaq (b), (c). Reprinted from Ref. 18. Copyright (2007), with permission from Elsevier.

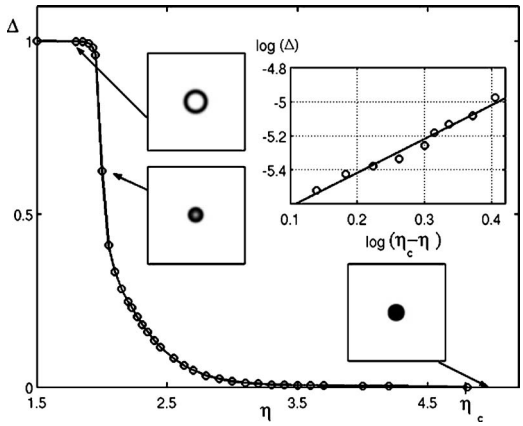

FIG. 8. Model calculations showing a transition from spots to rings as the lateral augmentation of the roots per unit biomass growth, η, decreases. The small insets show typical patch forms (at dimensional time $t=50$ years): spots at large η, latent rings at intermediate η, and visible rings at small η. The spots and latent rings are asymptotic forms while visible rings keep expanding. The larger inset shows a log-log plot supporting the scaling relation $\Delta\sim(\eta_c-\eta)^2$, where $\eta_c=4.8$. Parameters: $p=0.88$ (220 mm/yr), $\nu=4$, $\alpha=160$, $q=0.05$, $\rho=1$, $\gamma=5$, $f=0.1$, $\delta_b=0.02$, $\delta_w=2$, $\delta_h=200$. Reprinted from Ref. 18. Copyright (2007), with permission from Elsevier.

questions using the model Eqs. (1)–(4) with time-periodic precipitation rates, $p(t)$, representing seasonal rainfall variations. Specifically, a square-wave form, representing a four-month rainy period followed by an eight-month dry period, is chosen for $p(t)$.

To quantify the difference between spots and rings we introduce "ring index"[18] defined as

$$\Delta=\frac{b_{\max}-b_{\text{core}}}{b_{\max}}, \tag{5}$$

where $b_{\max}$ stands for the maximal biomass density in the patch and b_{core} for the biomass density in the patch center. The value $\Delta=0$ corresponds to a spot-like patch, where the maximal biomass density occurs at the core of the patch, $\Delta=1$ corresponds to a visible biomass ring ($b_{\text{core}}=0$), and intermediate values, $0<\Delta<1$, represent latent rings.

Since spot structures appear to be stabilized by the depletion of soil-water in the spot's surroundings, we chose to vary the parameter η which controls the root-system size and thus the water uptake in the vicinity of the spot. Figure 8 shows a graph of the ring index Δ as a function of η. At large η values the ring index vanishes, indicating the prevalence of stable spots. At small η values the ring index approaches unity, indicating the prevalence of visible rings. In between there is an η range of latent rings.

To better quantify the behavior near the transition point, $\eta=\eta_c$, from spots to latent rings we consider the core region where the biomass density can be expanded as $b(r)=b_{\text{core}}+a_2(\eta_c-\eta)r^2-a_4r^4+\cdots$. Here, r is the radial coordinate and a_2, a_4 are constants. A simple calculation shows that the ring index scales with the distance, $\eta_c-\eta$, from the transition point like $\Delta\sim(\eta_c-\eta)^2$, whereas the ring radius scales like $R\sim(\eta_c-\eta)^{1/2}$. The log-log plot inset in Fig. 8 supports these scaling relations. The scaling form for R is typical of instability phenomena. Numerical studies indeed show that small

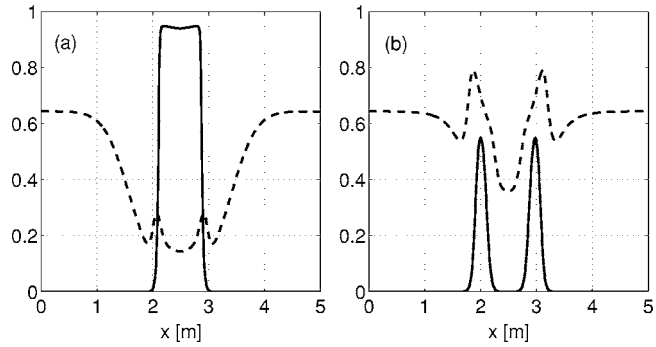

FIG. 9. Transects of two-dimensional spatial distributions of biomass and soil-water density for (a) a stationary spot solution ($\eta=3.2$), and (b) an expanding ring solution ($\eta=1.6$). Dimensional time is $t=50$ years and all other parameters are as in Fig. 8.

perturbations about spot solutions decay in time when $\eta>\eta_c$ but grow to form latent rings when $\eta<\eta_c$.

These results suggest the following mechanism of ring formation from small growing spots. A plant species characterized by a sufficiently large η, will deplete the soil-water density at the forefront of the growing spot to a level at which the spot can no longer expand, thus forming an asymptotic spot-like structure. In contrast, a small-η species, having a lower uptake rate, can keep expanding. The increased water stress at the spot's core will eventually lead to a central die-back and ring formation. Figure 9 shows biomass and soil-water profiles supporting this mechanism; the soil-water density at the forefront of a spot (ring) is significantly lower (higher) than the soil-water density in bare soil. Latent rings, like spots and unlike visible rings, approach asymptotic forms characterized by fixed averaged radii.

The results also suggest that ring-forming species all have compact root systems in the lateral directions. This appears consistent with the observation that all plant species showing ring formation expand vegetatively following "phalanx-growth" strategy.[18,27] In this strategy new individuals are added at the boundary of the biomass patch and are

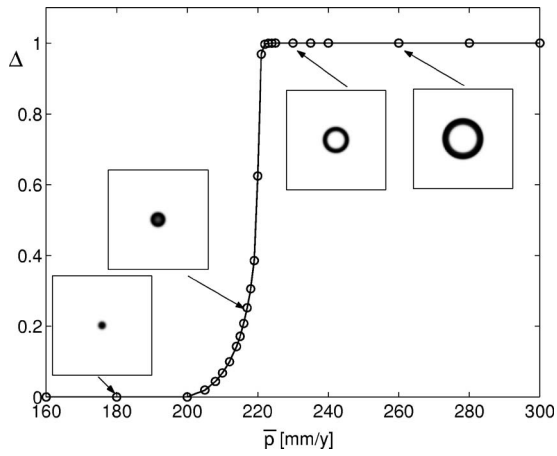

FIG. 10. Model calculations showing a transition from spots to rings as the mean annual precipitation rate, $\bar{p}$, increases. The insets show typical patch forms (at dimensional time $t=50$ years): spots at low $\bar{p}$, latent rings at intermediate $\bar{p}$, and visible rings at high $\bar{p}$. Parameters: $\eta=2$ and all other parameters are as in Fig. 8.

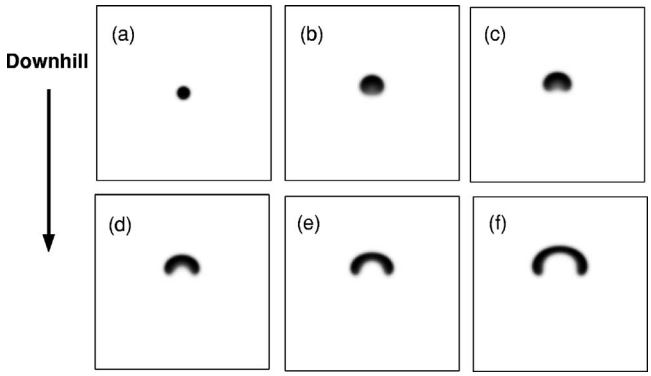

FIG. 11. Development of crescent patch forms on hill slopes. Snapshots of model simulations showing an initial spot evolving to form a crescent-like patch slowly migrating uphill. The times correspond to 2.5 yr (a), 15.5 yr (b), 22.5 yr (c), 30.5 yr (d), 37.5 yr (e), 49.5 yr (f). Parameters: $\eta=1.9$, slope$=2^{\circ}$ and all other parameters are the same as in Fig. 8.

connected to the clone by very short stems. This spatial expansion strategy results in highly dense patches of individuals whose roots are laterally confined.

For a given ring-forming species, characterized by some η value smaller that η_c, decreasing the mean annual precipitation rate $\bar{p}$, should result in the formation of a stable spot structure. This is because the soil-water density in the neighborhood of a small growing spot can drop below the level needed for its further expansion. As Fig. 10 demonstrates, a transition from rings to spots does occur by decreasing $\bar{p}$. Increasing the parameter f has a similar effect; higher f values imply higher infiltration rates in bare soil and lesser amounts of surface water accumulating at the vegetation spot. The instability threshold, η_c, therefore depends on $\bar{p}$, f and other parameters affecting the level of soil-water at the forefront of a vegetation spot.

The studies described so far apply to plane topography ($\nabla\zeta=0$). On a slope spots destabilize to crescent-like patches migrating uphill as Fig. 11 shows. The uphill part of the spot receives runoff generated by the large bare area uphill, while the downhill part receives a small amount of that runoff and loses runoff downhill. As a result the spot expands in the uphill direction and retreats in the downhill direction, forming a crescent patch form. Figure 12 shows a crescent patch form of *Asphodelus ramosus* on a slope observed in the northern Negev.

FIG. 12. A crescent-like patch of *Asphodelus ramosus* on a slope observed in the northern Negev (200 mm/yr). Typical patches are 20 cm long.

VI. ECOLOGICAL IMPLICATIONS

The studies of localized structures described in the previous sections have significant ecological implications in terms of habitat creation, by redistribution of the water resource, and in terms of resilience to environmental changes and disturbances, such as droughts and grazing. We briefly discuss these implications in the context of three topics of high current interest in ecology: facilitation by ecosystem engineers, species diversity along environmental gradients, and desertification.

A. Facilitation by ecosystem engineers

Plants are strongly affected by their physical (abiotic) environments, which determine the availability of crucial resources such as water, nutrients, and light. Plants also modify their abiotic environments, e.g., by soil-water uptake, nutrient consumption, shading of sunlight, or by changing infiltration rates. Some plant species, however, have more pronounced and significant effects on their abiotic environments than others. These species deserve special attention because of their potential ability to facilitate the growth of other species and thereby change species composition and richness. Species of this kind are often called "ecosystem engineers."[28–31]

In the context of dryland vegetation, ecosystem engineering is realized by the ability of woody plant species, such as certain shrubs, to concentrate the water resource in the vegetation patches they form. The significantly higher soil-water densities in these patches as compared with the density in the surrounding bare soil provide habitats for herbaceous species that cannot tolerate the water stress in bare soil.

The results shown in Fig. 4 point towards a plant trait that strongly affects the engineering capacity: the root-system augmentation in response to biomass growth, quantified by η. Plant species with smaller η concentrate more water and therefore are better ecosystem engineers. Figure 6 shows that a given ecosystem engineer may lose its engineering capacity when the precipitation rate p is increased, and Fig. 5 shows that the engineering capacity can be lost as a result of crust disturbances which increase the infiltration rate in bare soil (by increasing f).

All these factors, controlled by η,p,f, affect ecosystem engineering by changing the relative strengths of the infiltration and uptake processes. Dominance of the former favors water concentration and positive engineering whereas dominance of the latter favors water depletion and negative engineering.[32] Larger η values increase the water uptake process by extending the root system and therefore leads to negative engineering. Higher precipitation rates, p, significantly increase the patch size and therefore the number of individuals taking up water. The infiltration rate, on the other hand, increases only slightly, despite the increase of the biomass density, because of the weak biomass dependence of the infiltration rate at high biomass densities (see Fig. 1). As a result, increasing p tilts the water balance towards water uptake and negative engineering. Finally, higher f values increase the infiltration rate in bare soil and consequently re-

duce the flow of surface water into engineer's patches. As a result, the amount of surface water infiltrating into the soil within a patch decreases, which tilts the water balance towards negative engineering.

Crossovers from negative to positive engineering, or from competitive to facilitative interactions, in woody-herbaceous systems have recently been observed in field studies along rainfall gradients.[33,34]

B. Species diversity along environmental gradients

The dominant plant life-forms in drylands are woody and herbaceous vegetation. Because of water limitation typical landscapes are mosaics of woody patches and open nonwoody areas. Species diversity studies mostly focus on the herbaceous life form that can reside both in the woody patches and in the open areas, depending on the environmental conditions and the engineering capacity of the woody species.

The results presented in Fig. 6 suggest that at high precipitation rates herbaceous species will mostly occupy the open areas because the soil-water density there is higher than in woody patches, and can be above the tolerance limit to water stress. In contrast, at low precipitation rates herbaceous species may not tolerate the water stress in the open areas and will mostly reside in the mesic woody patches. This implies that species richness may not necessarily decline along the rainfall gradient, but species composition is expected to change because of the different environments woody patches and open areas provide. Shading-sensitive herbaceous species that occupy the open areas in high rainfall regions may disappear in low rainfall regions because the only areas that are mesic enough are the woody patches which block sunlight. In contrast, grazing-sensitive species that cannot tolerate the grazing stress in the open areas of high rainfall regions can colonize the woody patches in low rainfall regions because of the protection they provide. A recent study of a two-species version of the model equations, describing a woody-herbaceous system, confirms these expectations.[35]

The results presented in Fig. 5 suggest that gradients of soil conditions resulting in different infiltration rates can also affect species richness and/or composition. Regions subjected to grazing activity, for example, will suffer from broken soil-crust and consequently will experience higher infiltration rates (higher f values) in the open areas. While woody patches in undisturbed regions may show ring-like water distributions (Fig. 5, $f=0.04$), patches in moderately disturbed regions (Fig. 5, $f=0.12$) can show spot-like distributions. Thus, shading-sensitive species that cannot grow under the woody canopies in moderately disturbed regions, may appear at the peripheries of woody patches in undisturbed regions, where the soil-water density reaches its maximal value. In contrast, grazing-sensitive species that can grow under the woody canopies in moderately disturbed regions, may not be able to grow in undisturbed regions. Patches in highly disturbed regions (Fig. 5, $f=0.48$) may show no water concentration, and herbaceous vegetation may not grow at all.

The formation of biomass ring structures may have additional effects on species composition and richness, but we are not aware of empirical studies addressing this question.

C. Desertification

Desertification is defined as an irreversible decrease in biological productivity induced by an environmental change, and is captured by the model in bistability ranges of bare-soil and vegetation-pattern states, which are also the ranges where localized structures appear. One scenario of a desertification process is illustrated in Fig. 2.[5] A precipitation downshift to values below the threshold p_0 can induce a transition from the spot-pattern state, $\mathcal{S}$, to the bare-soil state, $\mathcal{B}$, because the former no longer exists at these precipitation values (see arrow in Fig. 2). The transition is irreversible because the bare-soil state remains stable even when the precipitation rate resumes its original value. Transitions of this kind are often referred to as "catastrophic regime shifts."[14,36] The same scenario represents desertification due to overgrazing, for grazing in the model is captured by the biomass-loss rate, M, which is inversely proportional to the dimensionless precipitation parameter p (see Table I).

Another scenario of desertification is illustrated in Fig. 5 with a species having low tolerance to water stress ($\eta=2$). A crust-removal disturbance that increases f beyond the threshold f_c results in a transition to the bare-soil state (because of the increased infiltration in bare soil and the corresponding decrease in surface water accumulating at the vegetation patch). The transition is irreversible because the bare-soil state remains stable even when the crust recovers.

VII. CONCLUSION

The model Eqs. (1)–(4) and their extension to multispecies plant communities[35] provide a theoretical platform for studying a variety of problems related to the patchiness, resilience, and diversity of dryland vegetation. A few such problems have been addressed in this paper, including (i) biomass-water relationships in spot-like vegetation patches, (ii) formation mechanisms of ringlike and crescent-like vegetation patches, (iii) resilience of vegetation patches to disturbances and precipitation downshifts, (iv) conditions for ecosystem engineering by plants, and (v) transitions from negative to positive engineering along environmental gradients and the implications to species-diversity change.

The results of these studies are consistent with field observations of transitions from competition to facilitation in woody-herbaceous systems along rainfall gradients,[33,34] with field observations of spot, ring, and crescent-like patches, and with the observation that rings in nature are formed by dense clonal plants. Theoretical results obtained with the same model equations for extended vegetation states[9–11] are also consistent with available field observations.[13–15] However, careful attempts to test theoretical predictions in controlled laboratory experiments are still scarce.[18] In particular, more effort is needed to resolve the soil-water distributions in vegetation patches, and to study their relations to the aboveground biomass distributions as the patches evolve in time, and under different environmental conditions.[17]

ACKNOWLEDGMENTS

We thank M. Shachak, A. Novoplansky, E. Sheffer, Y. Seligmann, J. von Hardenberg, and A. Provenzale for helpful discussions. This study has been supported by the James S. McDonnell Foundation and by the Center for Complexity Science.

[1]Drylands are water-limited systems comprising about 40% of the terrestrial earth surface.
[2]R. Lefever and O. Lejeune, Bull. Math. Biol. **59**, 263 (1997).
[3]O. Lejeune and M. Tlidi, J. Veg. Sci. **10**, 201 (1999).
[4]C. Klausmeier, Science **284**, 1826 (1999).
[5]J. von Hardenberg, E. Meron, M. Shachak, and Y. Zarmi, Phys. Rev. Lett. **87**, 198101 (2001).
[6]T. Okayasu and Y. Aizawa, Prog. Theor. Phys. **106**, 705 (2001).
[7]M. Rietkerk *et al.*, Am. Nat. **160**, 524 (2002).
[8]E. Meron, E. Gilad, J. von Hardenberg, M. Shachak, and Y. Zarmi, Chaos, Solitons Fractals **19**, 367 (2004).
[9]E. Gilad, J. von Hardenberg, A. Provenzale, M. Shachak, and E. Meron, Phys. Rev. Lett. **93**, 981051 (2004).
[10]H. Yizhaq, E. Gilad, and E. Meron, Physica A **356**, 139 (2005).
[11]E. Gilad, J. von Hardenberg, A. Provenzale, M. Shachak, and E. Meron, J. Theor. Biol. **244**, 680 (2007).
[12]M. Cross and P. Hohenberg, Rev. Mod. Phys. **65**, 851 (1993).
[13]C. Valentin, J. d'Herbès, and J. Poesen, Catalysis **37**, 1 (1999).
[14]M. Rietkerk, S. Dekker, P. de Ruiter, and J. van de Koppel, Science **305**, 1926 (2004).
[15]N. Barbier, P. Couteron, J. Lejoly, V. Deblauwe, and O. Lejeune, J. Ecol. **94**, 537 (2006).
[16]Various factors contribute to this effect, including biological crusts that grow on bare soil and reduce the infiltration rate, but do not develop in vegetation patches due to shading and litter formation, and soil mounds, formed by litter accumulation and dust deposition, that intercept runoff.
[17]F. Ludwig, H. de Kroon, F. Berendse1, and H. Prins, Ecology **170**, 93 (2004).
[18]E. Sheffer, H. Yizhaq, E. Gilad, M. Shachak, and E. Meron, "Why do plants in resource deprived environments form rings?" Ecol. Complexity (in press).
[19]We chose in this paper to view the closely related water-uptake and root-augmentation processes as two distinct feedbacks, one negative and one positive, rather than lumping them together under a single name, "uptake feedback," as we did in earlier publications (Refs. 9 and 11).
[20]B. Walker, D. Ludwig, C. Holling, and R. Peterman, J. Ecol. **69**, 473 (1981).
[21]S. Campbell, J. Seeler, and S. Glolubic, Arid Soil Res. Rehab. **3**, 217 (1989).
[22]The bifurcation is subcritical (supercritical) depending on whether the quantity $2\eta\nu/[\nu(1-\rho)+\gamma]$ is greater (lower) than unity.
[23]O. Lejeune, M. Tlidi, and P. Couteron, Phys. Rev. E **66**, 010901 (2002).
[24]F. Vasek, Am. J. Bot. **67**, 246 (1980).
[25]E. M. White, Rangelands **11**, 154 (1989).
[26]S. Wikberg and L. Mucina, J. Veg. Sci. **13**, 677 (2002).
[27]L. Lovett Doust, J. Ecol. **69**, 743 (1981).
[28]C. Jones, J. Lawton, and M. Shachak, Oikos **69**, 373 (1994).
[29]C. Jones, J. Lawton, and M. Shachak, Ecology **78**, 1946 (1997).
[30]K. Cuddington, J. Byers, A. Hastings, and W. Wilson, *Ecosystem engineers: Plants to protists* (Academic, New York, 2007).
[31]Ecosystem engineers need not necessarily be plant species. They can be micro-organisms such as cyanobacteria in drylands which reduce the infiltration rate of surface water by forming soil crusts, thereby increasing the flow of surface water into lower places. Ecosystem engineers can also be animals. A well known example is the North American beaver which forms small ponds by building dams across rivers.
[32]Positive (negative) engineering refers to situations in which the maximal soil-water density in the engineer's patch is higher (lower) than the soil-water density in bare soil.
[33]F. Pugnaire and M. Luque, Oikos **93**, 42 (2001).
[34]C. Holzapfel, K. Tielbörger, H. Paragb, J. Kigel, and M. Sternberg, J. Appl. Ecol. **7**, 268 (2006).
[35]E. Gilad, M. Shachak, and E. Meron, Theor Popul. Biol. **72**, 214 (2007).
[36]M. Scheffer, S. Carpenter, J. Foley, C. Folke, and B. Walkerk, Nature (London) **413**, 591 (2001).